water

MDPI

Article

Impacts of Climate and Land-Use Change on Blue and Green Water: A Case Study of the Upper Ganjiang River Basin, China

Yongfen Zhang [1,2], Chongjun Tang [2,*], Aizhong Ye [3], Taihui Zheng [2], Xiaofei Nie [2], Anguo Tu [2], Hua Zhu [4] and Shiqiang Zhang [1,*]

1 College of Urban and Environmental Science, Northwest University, Xi'an 710127, China; yongfenyk@stumail.nwu.edu.cn
2 Jiangxi Provincial Key Laboratory of Soil Erosion and Prevention, Jiangxi Institute of Soil and Water Conservation, Nanchang 330029, China; ztaihui@163.com (T.Z.); xfnie85@163.com (X.N.); tag20@163.com (A.T.)
3 Faculty of Geographical Science, Beijing Normal University, Beijing 100875, China; azye@bnu.edu.cn
4 Key Laboratory of Watershed Geographic Sciences, Nanjing Institute of Geography and Limnology, Chinese Academy of Sciences, Nanjing 210008, China; zhuhua18@mails.ucas.ac.cn
* Correspondence: tangchongjun@126.com (C.T.); zhangsq@nwu.edu.cn (S.Z.)

Received: 10 August 2020; Accepted: 22 September 2020; Published: 23 September 2020

Abstract: Quantitatively figuring out the effects of climate and land-use change on water resources and their components is essential for water resource management. This study investigates the effects of climate and land-use change on blue and green water and their components in the upper Ganjiang River basin from the 1980s to the 2010s by comparing the simulated changes in blue and green water resources by using a Soil and Water Assessment Tool (SWAT) model forced by five climate and land-use scenarios. The results suggest that the blue water flow (BWF) decreased by 86.03 mm year^{-1}, while green water flow (GWF) and green water storage (GWS) increased by 8.61 mm year^{-1} and 12.51 mm year^{-1}, respectively. The spatial distribution of blue and green water was impacted by climate, wind direction, topography, and elevation. Climate change was the main factor affecting blue and green water resources in the basin; land-use change had strong effects only locally. Precipitation changes significantly amplified the BWF changes. The proportion of surface runoff in BWF was positively correlated with precipitation changes; lateral flow showed the opposite tendency. Higher temperatures resulted in increased GWF and decreased BWF, both of which were most sensitive to temperature increases up to 1 °C. All agricultural land and forestland conversion scenarios resulted in decreased BWF and increased GWF in the watershed. GWS was less affected by climate and land-use change than GWF and BWF, and the trends in GWS were not significant. The study provides a reference for blue and green water resource management in humid areas.

Keywords: blue water; green water; SWAT; land use change; climate change; upper Ganjiang River basin

1. Introduction

In recent years, regional water cycle processes and the impacts on these processes from climate change have become topics of great academic interest [1,2]. Climate change can alter regional precipitation, temperature and evapotranspiration conditions, which then affects runoff and exacerbates water scarcities [3]. At the same time, as populations continue to grow, high-intensity human activities will alter land cover patterns, resulting in changes in water infiltration, evapotranspiration, and soil moisture conditions [4,5]. As a result of these factors, water resources will be redistributed in time and space, exacerbating the instability of water supplies and the conflict between water supply and demand [6]. Therefore, quantitative studies about the effects of climate and land-use change on water resources in time and space are of superb value to the rational development and utilization of water resources and the formulation of scientific management systems.

The concepts of blue and green water have provided new perspectives on water management in recent years [7–13]. These concepts were first introduced by Falkenmark [14]. Blue water is the sum of surface water (e.g., rivers, lakes, wetlands) and groundwater in liquid form. Green water is water from precipitation entering the soil that can be absorbed and utilized by plants. Green water includes green water flow (GWF) and green water storage (GWS). GWF is the actual evapotranspiration. GWS is the soil water content, which refers to water stored in the soil [11,15,16]. Traditionally, because blue water is directly related to human needs (drinking, irrigation, shipping, power generation, industrial production, etc.), most of the research on water resources has focused on blue water, while relatively little research has been performed on green water. In fact, green water is a large part of global water resources. Studies have shown that in humid areas, green water accounts for more than 30% of the total water resources. In arid areas, this proportion can reach more than 80% [8,17]. More importantly, green water is the basis for plant growth and plays an enormous part in both terrestrial ecosystems and rainfed agriculture [18]. Therefore, it is necessary to increase the amount of research on changes in green water resources. This topic is important for the efficient use of water resources, the promotion of food production security, and the maintenance of natural terrestrial ecosystems.

Research methods for green water have been growing in popularity as the concept of green water has gained more attention. Based on the definition of green water idea by Falkenmark, Rockström divided GWF into two indicators, the productive part (the actual transpiration) and the nonproductive part (the actual evaporation) of plant biomass [11]. Kui Zhu refined the quantitative evaluation of green water by proposing new indicators [19]. In addition, the water footprint is an important aspect of green water research [20,21]. According to Zhao, climate change is the main factor influencing water resource changes in large watersheds, and dramatic changes in land-use modes play a key role in the water cycle of small watersheds [8]. However, research on the response of each component of blue and green water to climate and land-use change is relatively scarce. There is also a lack of research on the possible impacts of government decisions on regional blue and green water resources. The differences between this paper and other similar studies are as follows. (1) The responses of each component of blue and green water to climate and land-use change were studied quantitatively. Consumed green water (CGW) was introduced into the GWF, and surface runoff (SURQ), groundwater flow (GWQ), and lateral flow (LATQ) were introduced into the blue water flow (BWF). This method is more refined than the analyses in previous studies. (2) The potential impacts on the regional blue and green water resources and their components were analyzed in the context of China's policy of returning farmland to forests.

The Ganjiang River is an important tributary of the Yangtze River. It belongs to the humid region of southeastern China. Since the 1980s, under the influence of global climate change, the uneven temporal distribution of precipitation in the Ganjiang River basin has increased, consequently increasing the risk of droughts and floods [22]. Due to rapid urbanization, large-scale afforestation and other soil and water conservation projects, and the policy of returning farmland to forests, land-use patterns in the upper Ganjiang River basin have undergone relatively large changes [23,24]. It is unclear how the region's blue and green water have changed under the combined influence of these factors. Thus, this area provides a representative study area for us to carry out research on the impacts of climate and land-use change on blue and green water. The main contents of this paper are as follows. The primary goals of this study are (1) to simulate the hydrological processes in the upper Ganjiang River basin using the Soil and Water Assessment Tool (SWAT) model based on parameter sensitivity analysis and data calibration and validation; (2) to quantify the characteristics of the effects of climate and land-use change on blue and green water and their components in time and space; and (3) to design multiple scenarios to study the characteristics of blue and green water and their components under different meteorological conditions and land-use scenarios.

2. Materials and Methods

2.1. Study Area and Datasets

2.1.1. Study Area

The Ganjiang River originates in the southern part of Jiangxi Province and flows from southern to northern into Poyang Lake (China's largest freshwater lake). The Ganjiang River is 823 km long, and its upper reaches are located above the Dongbei hydrological station. The upper Ganjiang River basin is located between 113°30′ E–116°40′ E, 24°26′ N–27°07′ N (Figure 1). The upper basin covers an area of 40,564 km^2, accounting for 48% of the total area of the Ganjiang River basin. The basin experiences a subtropical monsoonal humid climate with an annual precipitation of 1400–2000 mm, which shows obvious interannual variation and uneven distribution throughout the year. The flood season is from April to September of each year. The precipitation during this period accounts for 65% to 70% of the total annual precipitation. The average temperature throughout the year is 17–26 °C. The main soil type is red soil, which is an acidic soil that is rich in iron and aluminum oxides that forms in humid climates [25]. The region is a globally important producer of navel oranges. The terrain in this area is dominated by low mountains and hills.

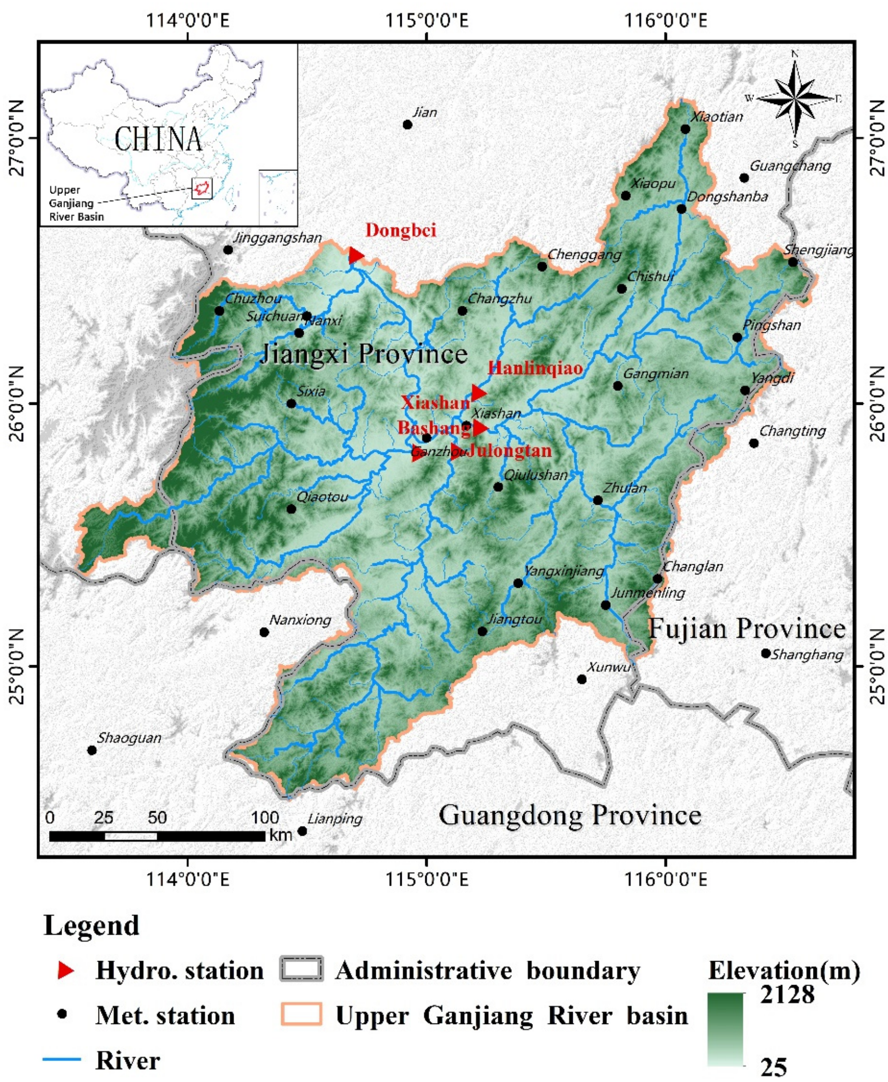

Figure 1. The position of the upper Ganjiang River basin and the distribution of hydrological and meteorological stations.

2.1.2. Data

Meteorological data were collected from 32 meteorological (rainfall) stations in around the upper Ganjiang River basin from 1975 to 2015. Daily precipitation, maximum/minimum temperature, relative humidity, and wind speed data for 12 meteorological stations were collected from the China Meteorological Data Service Center (http://data.cma.cn). Daily precipitation data for 30 rainfall stations were collected from the Jiangxi Hydrology Bureau (Figure 1). The ASTER GDEM dataset (30 m × 30 m) was supplied by way of the Geospatial Data Cloud site, Computer Network Information Center, Chinese Academy of Sciences (http://www.gscloud.cn). The 1980 and 2010 land-use data (30 m × 30 m) were obtained from the Resource and Environment Data Cloud Platform, Chinese Academy of Sciences (http://www.resdc.cn) (Figure 2). Based on the input data requirements of the SWAT model, the two periods of land-use data were reclassified by merging similar land-use types. The reclassified land-use types included forest, agricultural land, pasture, water, and built-up land. The Harmonized World Soil Database (HWSD_v121) in SWAT format (1 km × 1 km) was obtained from the Water Weather Energy Ecosystem Technology and Data website, 2w2e Gmbh (https://www.2w2e.com/). Monthly flow data for the five hydrological stations at Hanlinqiao, Xiashan, Julongtan, Bashang, and Dongbei were obtained from the Jiangxi Provincial Hydrological Bureau (Figure 1).

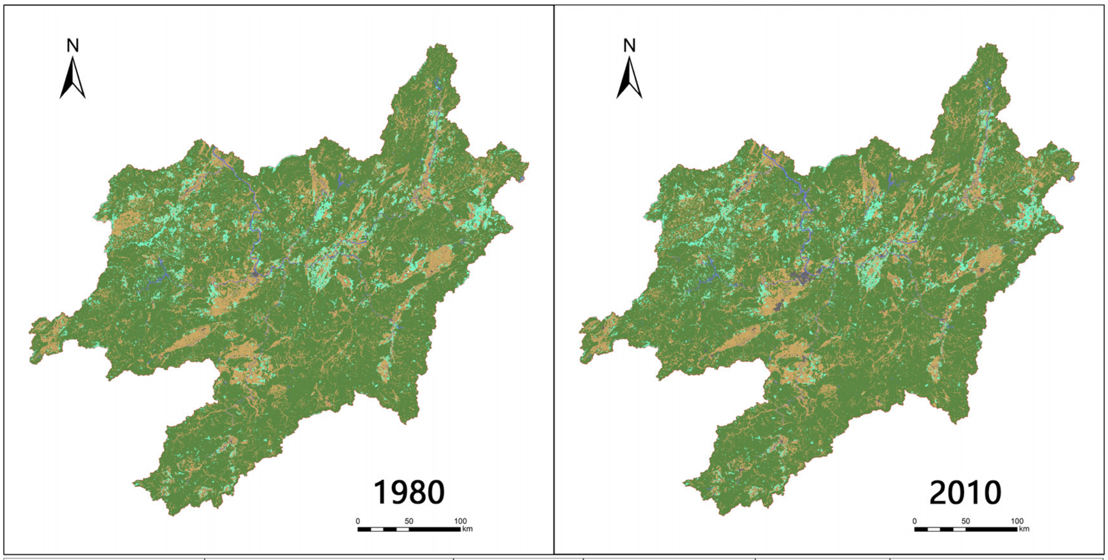

Land use	Agricultural land	Forest	Grassland	Water	Built-up land
1980 (km^2)	7577.11	29623.13	2597.86	411.66	351.43
2010 (km^2)	7497.68	29537.62	2579.27	456.22	490.63
% Change in area	−1.05	−0.29	−0.72	10.83	39.61

Figure 2. Land-use distribution and changes in the upper Ganjiang River basin, 1980 and 2010.

2.2. *Methodologies*

2.2.1. SWAT Model

The SWAT model, a semi-distributed hydrological model suitable for large basins, was developed by the USDA Agricultural Research Service in the 1990s on the basis of the Simulator for Water Resources in Rural Basins (SWRRB) model, which has been widely used in studies in different parts of the world [26–30]. It provides a simulation of the hydrology and associated material transport transformations in a watershed by integrating the watershed's topography, soils, land use, weather, and land management practices [30]. The model can divide the watershed into subbasins based on Digital Elevation Model (DEM) data, and each subbasin is subdivided into smaller hydrological response units (HRUs) based on the slope, land-use type, and soil type. HRU is the basic unit for hydrological calculations in the SWAT model. The model calculates the evapotranspiration, infiltration and other parameters for each HRU and then sums the corresponding parameters from each HRU to obtain the evapotranspiration, surface runoff, and other hydrological variables for each subbasin [31]. The hydrological cycle in the SWAT model is based totally on the water balance equation, which is expressed as follows:

$$SW_t = SW_0 + \sum_{i=1}^{t} \left(R_{day} - Q_{surf} - E_a - W_{seep} - Q_{gw} \right) \quad (1)$$

where SW_t is the final soil water content (mm); SW_0 is the preliminary soil water content (mm); t is the time step (d); R_{day}, Q_{surf}, and E_a are the amounts of precipitation, surface runoff, and evaporation on day i (mm), respectively; W_{seep} is the amount of water entering the vadose zone from the soil profile on day i (mm); and Q_{gw} is the amount of the return flows on day i (mm).

Based on the results of previous studies [19], the relationship between blue and green water and their respective components in this study is expressed as follows:

$$\text{BWF} = \text{SURQ} + \text{LATQ} + \text{GWQ} \quad (2)$$

$$\text{GWF} = \text{CGW} + \text{NGW} \quad (3)$$

where BWF is the blue water flow (mm), the total volume of water entering the river from the HRU to the subbasin during the time step; SURQ, LATQ, and GWQ are the surface runoff, lateral flow, and groundwater flow, respectively, that flow into the channel over the time step (mm); GWF is the green water flow, the actual amount of evapotranspiration over the time step (mm); CGW is the consumed green water, the amount of evapotranspiration from farmland, grassland, and forestland (mm); NGW is the nonutilized green water, the amount of evapotranspiration from cities and water bodies (mm) [19]; and GWS is the green water storage and indicates the soil water content (SW), i.e., the amount of water stored in the soil profile over the time step (mm).

The sequential uncertainty fitting (SUFI-2) method in the SWAT Calibration and Uncertainty Program (CUP) was used for model calibration and validation, using the P-factor and R-factor to measure the effects of model rate-setting and uncertainty analysis [32]. The P-factor represents the percentage of observed data enveloped by the modeling result, the 95 PPU (95% prediction uncertainty), and the R-factor represents the mean width of the 95 PPU interval divided by the standard deviation of the measured data. In general, the closer the P-factor is to 1 and the closer the R-factor is to 0, the closer the simulation is to the true value. The uncertainty of the simulation is considered acceptable when the P-factor > 0.5 and R-factor < 1.5; when the P-factor > 0.7 and R-factor < 1, the uncertainty of the simulation is low [29]. The coefficient of determination (R^2) and the Nash–Sutcliffe coefficient (NS) were used in this paper to evaluate the applicability of the SWAT model. R^2 indicates the consistency of the trends between the simulated and measured values. A value closer to 1 means that the simulated values are more consistent with the measured values. $R^2 > 0.6$ is usually used as a criterion for the degree of correlation between the measured and simulated values. NS indicates the degree of deviation of the measured value from the simulated value. The closer the value is to 1, the smaller the deviation between the simulated and measured values. When NS ≤ 0.36, the simulation is considered to be unsatisfactory. When 0.36 < NS < 0.75, the simulation is considered to be good. When NS ≥ 0.75, the simulation is considered to be excellent [33].

2.2.2. Scenario Simulation

Based on the calibration and the validation of the SWAT model, this study simulated the main factors affecting the blue and green water resources in the upper Ganjiang River basin from 1980 to 2009 by holding the other factors fixed and varying only the land use or meteorological conditions. Five scenarios were simulated in total.

Scenario I: Land use in 1980 and meteorological conditions from 1976 to 1984.

Scenario II: Land use in 1980 and meteorological conditions from 2006 to 2015.

Scenario III: Land use in 2010 and meteorological conditions from 2006 to 2015.

Scenario IV: Based on Scenario III, nine climate change scenarios were designed that simulated temperature increases of 1, 2, and 3 °C, precipitation decreases of 10%, 20%, and 30%, and precipitation increases of 10%, 20%, and 30%.

Scenario V: Based on Scenario III, four scenario models were designed that take into account the implementation requirements of the latest policy for returning agricultural land to forests in China. The two normal scenarios simulate the conversion of agricultural land with slopes above 25° and above 15° to forestland. The two extreme scenarios simulate the conversion of all agricultural land to forestland and the conversion of all forestland to agricultural land.

In the scenario models above, the changes in blue and green water resources in the upper reaches of the Ganjiang River basin can be calculated as Scenario II–Scenario I, Scenario III–Scenario II, and Scenario III–Scenario I under the influences of climate change, land-use change, and their combined factors, respectively. Scenarios IV and V allow more extensive quantitative differentiation of the effects of precipitation and temperature changes on blue and green water, as well as the effects of conversions between agricultural land and forestland. The calculations of blue water and green water were based on multiyear averages. For example, the amount of water in the 1980s was the annual average from 1976–1985, and the amount of water in the 2010s was the annual average from 2006–2015

3. Results

3.1. Calibration and Validation

In establishing the simulation period, this study used a sectional approach based on the land-use scenarios in 1980 and 2010 to make the simulation results more realistic. The land-use scenarios were divided into periods as follows: (1) 1980 land-use scenario: warm-up period 1975–1977, calibration period 1978–1980, and validation period 1981–1983; (2) 2010 land-use scenario: warm-up period 2005–2007, calibration period 2008–2010, and validation period 2011–2013; (3) 2010 land-use scenario: warm-up period 2005–2007, calibration period 2008–2010, and validation period 2011–2013; and (4) 2010 land-use scenario: warm-up period 2005–2007, calibration period 2008–2010, and validation period 2011–2013.

Sixteen parameters (Table 1) were selected for further model calibration in each subbasin of this study based on the results of previous studies. Then, the observed monthly runoff data from 1978–1983 and 2008–2013 from the five hydrological stations at Hanlinqiao, Xiashan, Bashang, Julongtan, and Dongbei were used to perform the uncertainty analysis, calibration, and validation of the SWAT model output for the relevant subbasins based on the SUFI-2 method in the SWAT-CUP tool. The results showed that the uncertainties of the simulations for all hydrological stations except Dongbei were very low. At the Dongbei hydrological station, the P-factor was greater than or equal to 0.5 in both historical periods, which is also an acceptable degree of uncertainty. In terms of the simulation effect, the R^2 for both historical scenarios at the five hydrological stations was greater than 0.8 regardless of the rate period or the validation period, indicating that the trends in the simulated and measured values are highly consistent. The NS values for all hydrological stations in each scenario for both the rate period and the validation period were above 0.6, indicating a "good" to "excellent" simulation (Table 2). The results of these statistical analyses indicate that the SWAT model is applicable for the simulation of hydrological processes in the upper Ganjiang River basin and that this model can be used in further research (Figure 3).

Table 1. The parameters for model calibration and validation and their maximum theoretical range.

Parameter	Description	Maximum Theoretical Range
CN2	Soil Conservation Service (SCS) runoff curve number	35–98
USLE_P	Universal soil loss equation (USLE) equation support practice factor	0–1

Table 1. *Cont.*

Parameter	Description	Maximum Theoretical Range
GW_DELAY	Groundwater delay (day)	0–500
GWQMN	Threshold water depth in the shallow aquifer required for return flow to occur (mm)	0–5000
GW_REVAP	Groundwater "revap" coefficient	0.02–0.2
RCHRG_DP	Deep aquifer percolation fraction	0–1
REVAPMN	Threshold water depth in the shallow aquifer for "revap" or percolation to the deep aquifer to occur (mm)	0–500
CH_N2	Manning's "n" value for the main channel	−0.01–0.23
CH_K2	Hydraulic conductivity in the main channel alluvium (mm/h)	−0.01–500
SOL_AWC	Available soil water content (mm/mm)	0–1
SOL_K	Saturated hydraulic conductivity (mm/h)	0–2000
SOL_ALB	Moist soil albedo	0–0.25
ESCO	Soil evaporation compensation factor	0–1
SLSUBBSN	Average slope length (m)	10–150
CANMX	Maximum canopy storage (mm)	0–100
EPCO	Plant uptake compensation factor	0–1

Table 2. Results of uncertainty analyses and evaluations of the simulations under two historical scenarios, 1980 and 2010, at each hydrological station.

Station	Land-Use Scenario	Calibration and Validation	P-Factor	R-Factor	R^2	NS
HanLinqiao	1980	Calibration (1978–1980)	0.86	0.71	0.94	0.91
		Validation (1981–1983)	——	——	0.96	0.95
	2010	Calibration (2008–2010)	0.81	0.83	0.93	0.85
		Validation (2011–2013)	——	——	0.88	0.78
XiaShan	1980	Calibration (1978–1980)	0.93	0.68	0.97	0.91
		Validation (1981–1983)	——	——	0.92	0.90
	2010	Calibration (2008–2010)	0.78	0.80	0.94	0.83
		Validation (2011–2013)	——	——	0.95	0.62
JuLongtan	1980	Calibration (1978–1980)	0.94	0.60	0.96	0.92
		Validation (1981–1983)	——	——	0.94	0.92
	2010	Calibration (2008–2010)	0.78	0.79	0.95	0.86
		Validation (2011–2013)	——	——	0.94	0.79
BaShang	1980	Calibration (1978–1980)	0.86	1.18	0.89	0.72
		Validation (1981–1983)	——	——	0.92	0.82
	2010	Calibration (2008–2010)	0.92	1.30	0.92	0.90
		Validation (2011–2013)	——	——	0.89	0.87
DongBei	1980	Calibration (1978–1980)	0.50	0.44	0.87	0.80
		Validation (1981–1983)	——	——	0.85	0.82
	2010	Calibration (2008–2010)	0.53	0.50	0.85	0.72
		Validation (2011–2013)	——	——	0.83	0.72

3.2. *Impacts of Climate and Land-Use Change on Blue Water Flow*

Due to the combined effects of land-use change and climate change, the BWF in the upper Ganjiang River basin decreased by 86.03 mm, from 1055.38 to 969.35 mm, between the 1980s and the 2010s (Scenario III–Scenario I). Of the BWF components, SURQ accounted for the largest proportion of the total BWF, approximately 48–51%, followed by GWQ (35–38%) and LATQ. However, of the magnitudes of the decreases in these components, GWQ had the largest change with a decrease of 63.03 mm year^{-1}, followed by SURQ (decrease of 12.8 mm year^{-1}) and LATQ (decrease of 10.2 mm year^{-1}). This means that the GWQ is more affected by land-use change and climate change than the SURQ. LATQ is a generally stable component of BWF. The BWF in the upper Ganjiang River basin decreased by 85.96 mm year^{-1} (Scenario II–Scenario I) and by 0.07 mm year^{-1} (Scenario III–Scenario II), respectively, when only the individual influences of climate and land-use change were considered. This indicates that climate change affects blue water much more than land-use change. The trends in SURQ, GWQ, and LATQ due to climate change were generally consistent with trends in the BWF. Land-use change had minimal effects on the BWF, but its effects on the components of the BWF differed from the effects of climate change in that SURQ and GWQ decreased by 0.22 mm and by 0.48 mm year^{-1}, respectively, while LATQ increased by 0.63 mm year^{-1} (Figure 4).

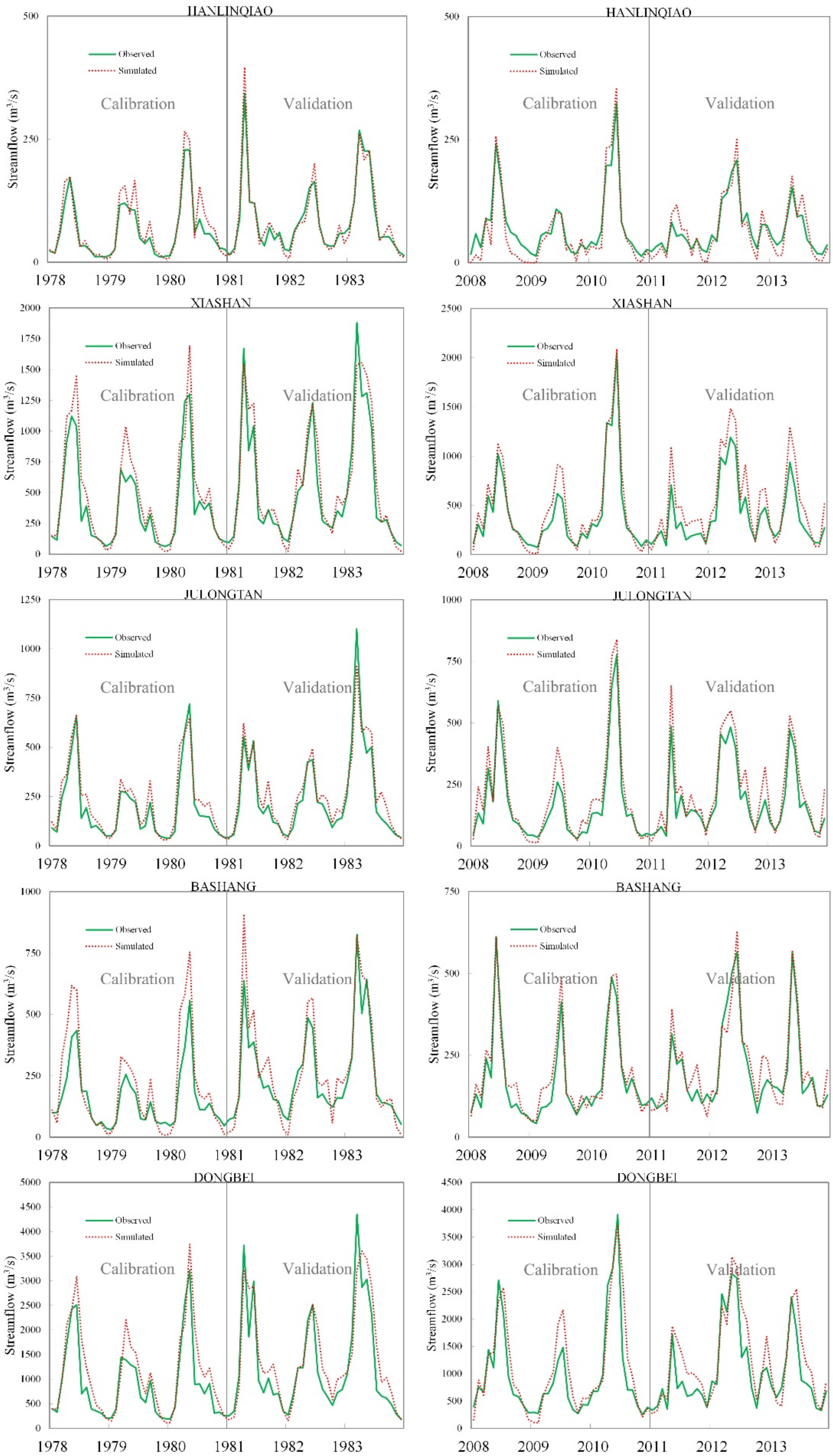

(**a**) (**b**)

Figure 3. Comparison of 1980 (**a**) and 2010 (**b**) observed and simulated runoff at five hydrological stations (Hanlinqiao, Xiashan, Bashang, Julongtan, and Dongbei) under land-use scenarios.

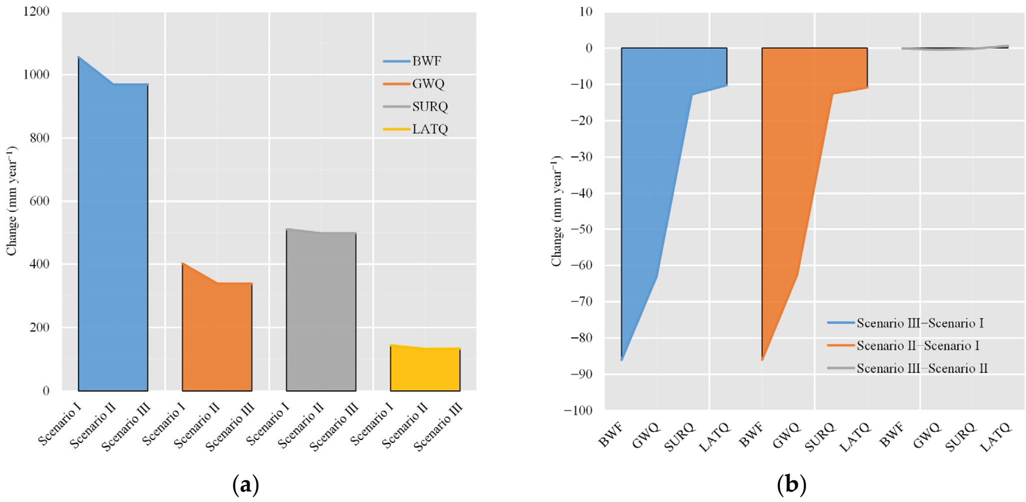

Figure 4. Simulation of the average annual values of blue water flow (BWF) and its components (surface runoff (SURQ), lateral flow (LATQ), groundwater flow (GWQ)) (**a**) in the upper Ganjiang River basin due to climate change, land-use change, and the combined effects of all the above factors (**b**).

In terms of spatial distribution, the BWF in the three scenarios was high around the watershed and low in the center of the watershed, with the BWF in the eastern and southeastern regions being higher than that in the western and central regions (Figure 5). This may be related to the varied topography of the upper Ganjiang River basin. When moisture from the East Asian monsoon flows into the region, it is first blocked by the surrounding mountains and forms precipitation. The central region is relatively weakly affected by this phenomenon, and the intensity of precipitation has a corresponding effect on the BWF. Under the influence of climate change, the BWF increased in the northern part of the basin and decreased in the southern part to varying degrees. Land-use changes had little impact on the BWF in the upper Ganjiang River basin, with changes ranging from −15 to 15 mm year^{-1} in all areas except the Ganzhou urban area. This was due to the increase in impervious areas associated with urban expansion, which resulted in a significant increase in BWF in this small region.

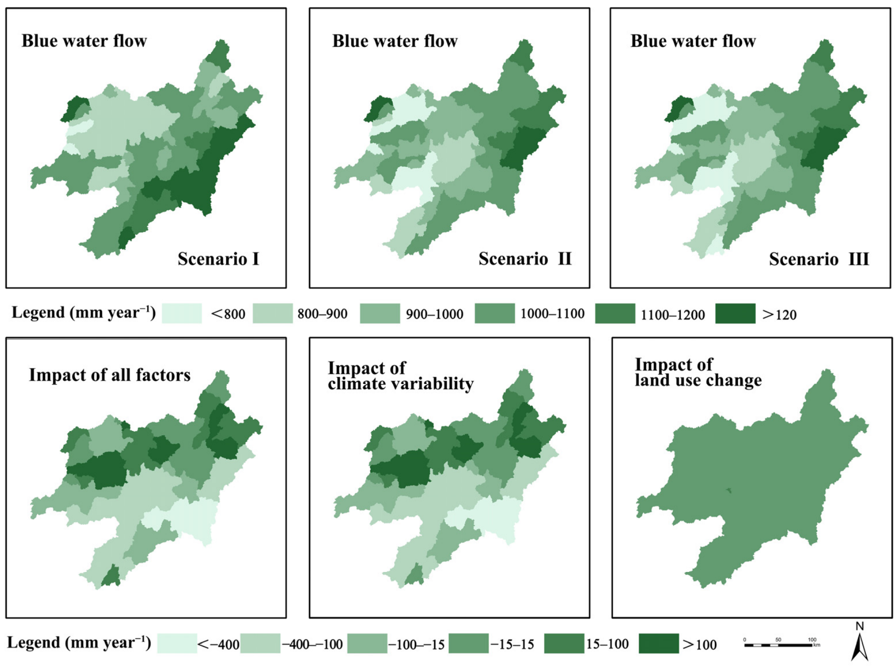

Figure 5. Spatial distribution of BWF and changes in BWF in the upper Ganjiang River basin under the individual or combined influence of climate and land-use change.

3.3. Impacts of Climate and Land-Use Change on Green Water Flow

The GWF in the upper Ganjiang River basin was approximately 600 mm $year^{-1}$ under the three scenarios (Figure 6). In contrast with the decreasing trend in BWF, climate change increased the watershed GWF by 8.61 mm $year^{-1}$ (Scenario II–Scenario I), while land-use change increased the GWF by only 0.01 mm $year^{-1}$ (Scenario III–Scenario II). The changes in CGW influenced by climate change showed the same trends as the changes in GWF, increasing by 8.59 mm $year^{-1}$. In contrast, CGW was reduced by 0.48 mm $year^{-1}$ by land-use change, suggesting that although land-use change had little effect on the watershed GWF, the increase in urban land use reduced the watershed CGW to some extent.

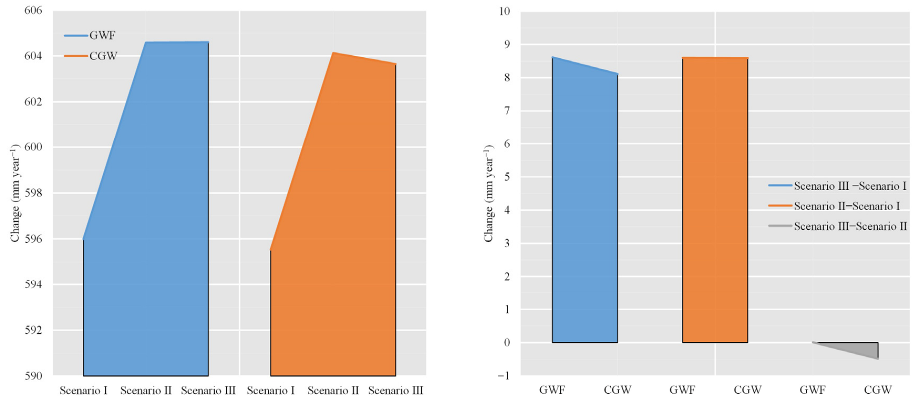

(**a**) (**b**)

Figure 6. Simulation of the average annual values of green water flow (GWF) and its components (consumed green water, or CGW) (**a**) in the upper Ganjiang River basin due to climate change, land-use tchange, and the combined effects of all the above factors (**b**).

In terms of spatial distribution, the GWF showed low values in the southeast and high values in the northwest in all three scenarios. Climate change increased the GWF in the eastern and northwestern parts of the basin, while it decreased the GWF in the central and southwestern parts of the basin. Some regions, including the Ganzhou urban area, experienced very significant increases or decreases in GWF that were associated with the dramatic variations in land-use change in these regions (Figure 7).

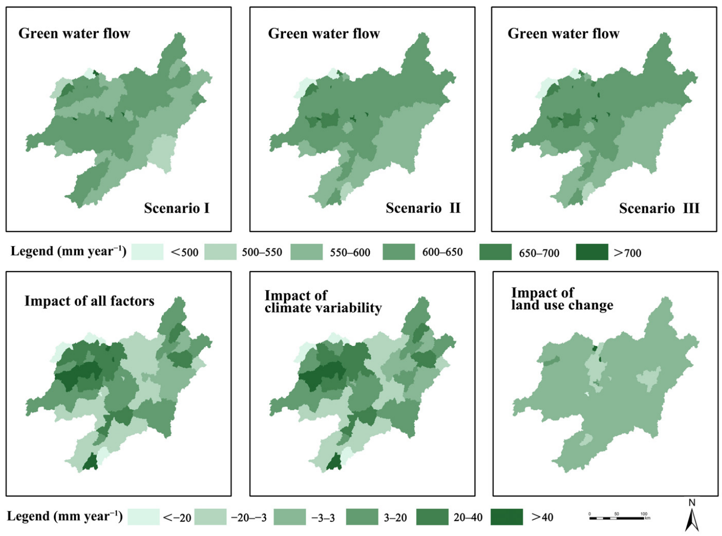

Figure 7. Spatial distribution of GWF and change in GWF in the upper Ganjiang River basin under the individual or combined influence of climate and land-use change.

3.4. Impacts of Climate and Land-Use Change on Green Water Storage

The trend in GWS variation is consistent with that in GWF variation. Due to the combined effects of climate and land-use change, the GWS in the upper Ganjiang River basin increased by 12.51 mm year^{-1}, from 105.33 (Scenario I) to 117.84 mm year^{-1} (Scenario III). Climate change increased the GWS by 12.64 mm year^{-1}, and land-use change decreased it by 0.13 mm year^{-1} (Figure 8). The spatial distribution of watershed GWS was positively correlated with elevation; higher-elevation regions had relatively higher GWS. Climate change caused the GWS to increase to different degrees in the region, with increases ranging from 2 to 24 mm year^{-1}, and the northeastern, southwestern, and western regions showed greater increases than the other regions (Figure 9). Notable conversions between built-up and non-built-up land (cropland, woodland, and grassland) in part of the region resulted in a significant change in the GWS in the region. The conversion of non-built-up land to built-up land led to a decrease in GWS and vice versa.

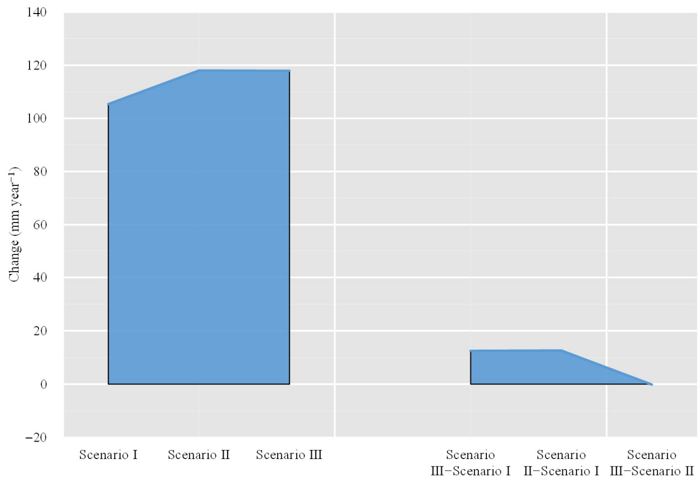

Figure 8. Simulation of the average annual values of GWS in the upper Ganjiang River basin due to climate change, land-use change, and the combined effects of all the above factors.

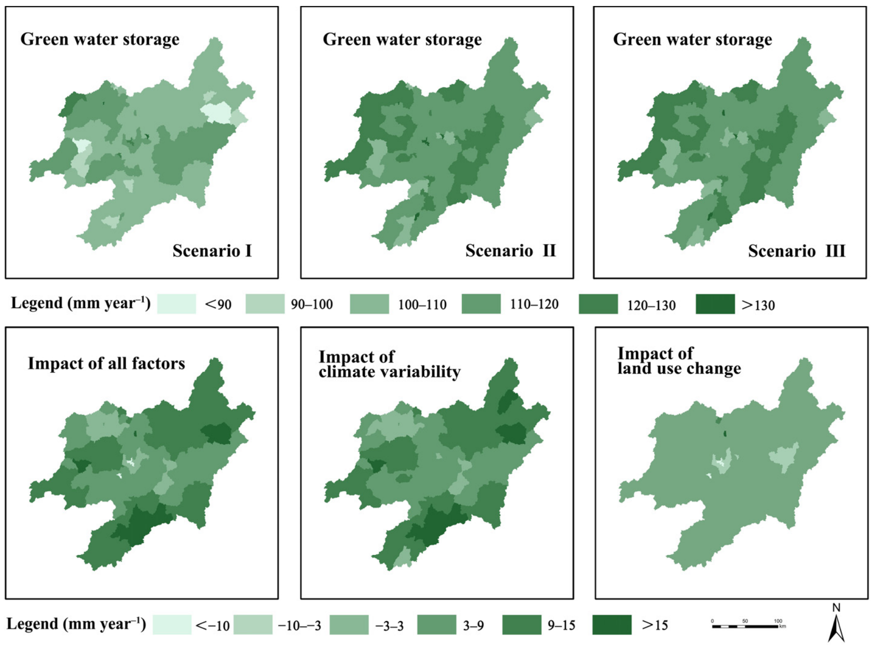

Figure 9. Spatial distribution and change in GWS in the upper Ganjiang River basin under the individual or combined influence of climate and land-use change.

3.5. Impacts of Changing Climate Factors on Blue Water and Green Water

Using Scenario III as a baseline, the effects on blue water and green water in the basin were studied by changing the climate factors (Figure 10). The trend in BWF was the same as that in precipitation: when precipitation increased, BWF increased, and vice versa. The BWF increased by 9.81%, 25.41%, and 41.5% when the precipitation increased by 10%, 20%, and 30%, respectively. The BWF decreased by 21.41%, 36.92%, and 51.74% when the precipitation decreased by 10%, 20%, and 30%, respectively, and these decreases in BWF were significantly higher than the corresponding decreases in precipitation. The BWF decreased by 6.82%, 7.63%, and 8.53% when the air temperature increased by 1, 2, and 3 °C, respectively. This demonstrated that the increase in evapotranspiration due to higher temperatures was accompanied by a decrease in the BWF. In addition, of all the tested temperature increases, the BWF was the most sensitive to the temperature increase up to 1 °C.

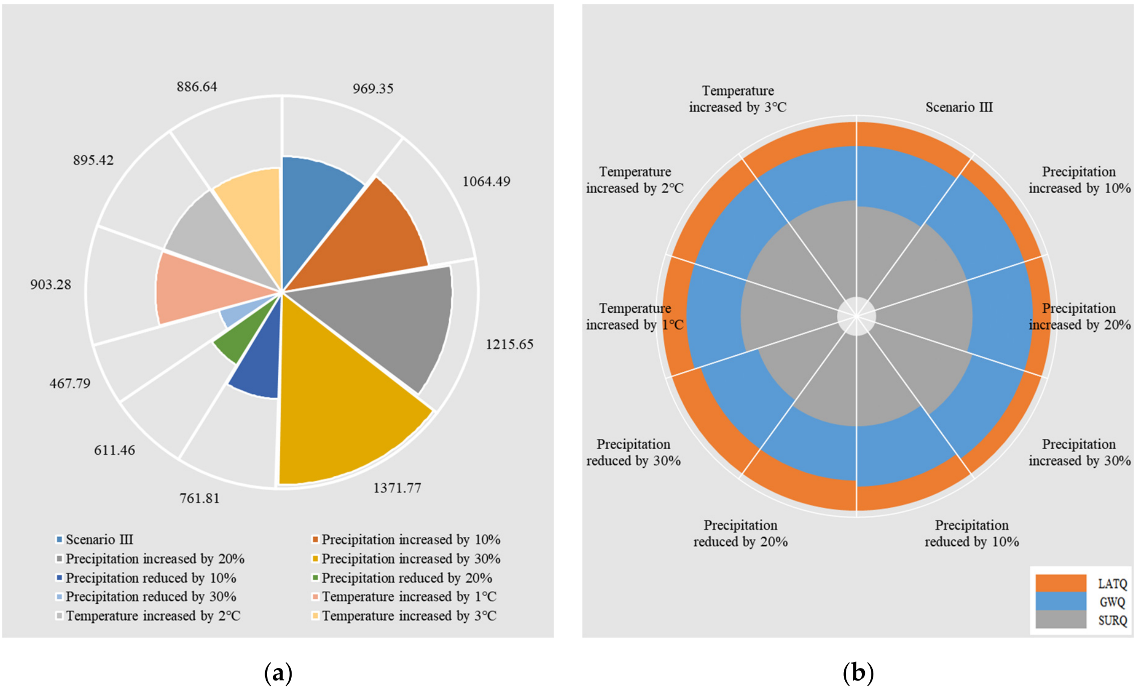

Figure 10. Simulation of the annual mean values (mm year^{-1}) of BWF (**a**) and the proportions of its components (SURQ, LATQ, GWQ) (**b**) in the upper Ganjiang River basin by individual altered precipitation and temperature factors based on Scenario III.

Of the various components of the BWF, SURQ accounted for the largest proportion of the total BWF, between 48% and 56%; GWQ accounted for approximately 31% to 34% of the total BWF, and LATQ made up the smallest proportion, accounting for approximately 11% to 19% of the total BWF. As the precipitation increased, the proportion of SURQ also increased, the proportion of LATQ decreased, and the proportion of GWQ was relatively stable. As the precipitation decreased, the proportion of SURQ decreased, the proportion of LATQ increased, and the proportion of GWQ was relatively stable. This indicates that among the components of blue water, surface runoff responds more positively than the other components to precipitation. The effect of increasing the temperature on each component of the BWF was small. The proportion of SURQ showed a weak upward trend with increasing temperature; the proportion of GWQ showed a weak downward trend, both increasing and decreasing within 1%; and LATQ remained relatively stable.

The changes in GWF and CGW were consistent with the increasing and decreasing trends in precipitation, with increases in GWF ranging from 10.88% to 12.59% and decreases in GWF ranging from 8.52% to 4.69%. The increase in GWF with precipitation is smaller than the decrease in GWF with precipitation. The increase in temperature led directly to an increase in evapotranspiration (GWF) that ranged from 10.85% to 13.5%. Of all the tested temperature increases, GWF was the most sensitive to the increase in temperature of up to 1 °C. The responses of GWS to changes in precipitation and temperature were relatively stable but still positively correlated, with increases in GWF within 1.41% and decreases ranging from 2.49% to 8.44%. With the increasing temperature and the corresponding increase in evapotranspiration, there was a decreasing trend in GWS, ranging from 1.37% to 2.24% (Figure 11).

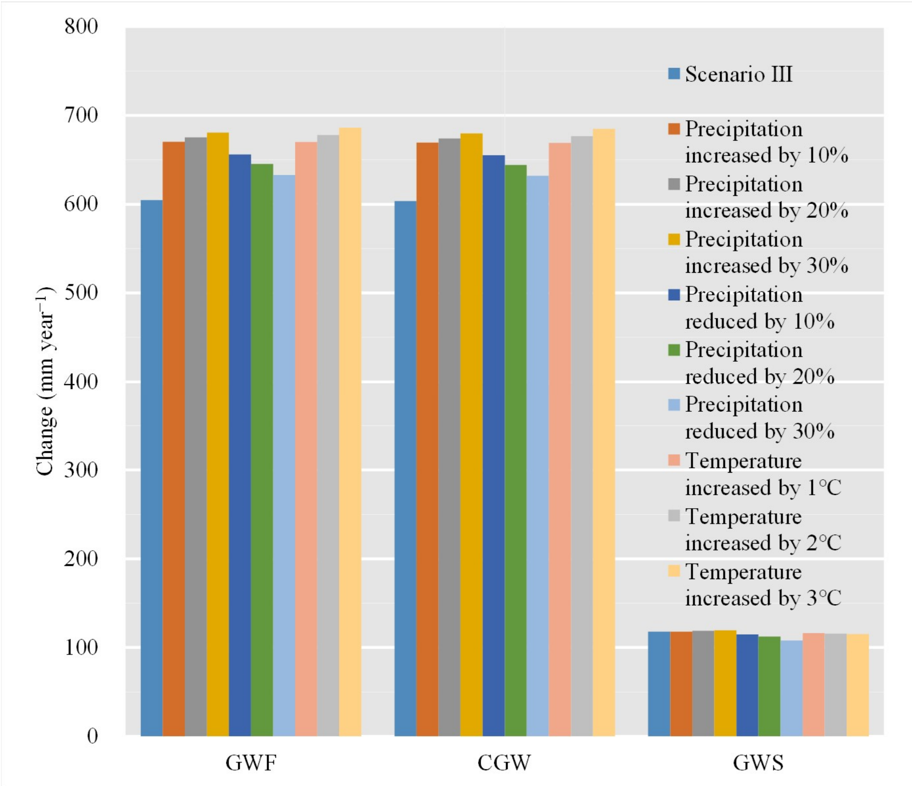

Figure 11. Simulation of the annual mean values of GWS, GWF, and its components (CGW) in the upper Ganjiang River basin by individually altered precipitation and temperature factors based on Scenario III.

3.6. Impacts of Land-Use Factor Changes on Blue Water and Green Water

Overall, based on Scenario III, all agricultural and forestland conversion scenarios resulted in a decrease in BWF and an increase in GWF in the basin. The BWF decreased by 6.4%, 6.08%, and 7.44% and the GWF increased by 10.14%, 9.7%, and 11.48%, respectively, in the upper Ganjiang River basin when agricultural land with slopes above 25° or 15° or all agricultural land was converted to forestland. Among the BWF components, as the proportion of cropland converted to forestland increased, the proportion of SURQ in the BWF experienced an increase and then a decrease, from 51% in the initial state (Scenario III) to 53% when agricultural land on slopes above 15° was converted to forestland and then to 48% when all agricultural land was converted to forestland. In contrast, the proportion of GWQ decreased and then increased, with the same magnitude of change as observed for SURQ, and the proportion of LATQ in the BWF remained stable. When all forestland was converted to agricultural land, the BWF decreased by 1.45%, and the GWF increased by 3.68%. The proportion of SURQ in the BWF increased to 72%, while those of GWQ and LATQ decreased to 19% and 9%, respectively. The GWS decreased by 1.22%, 1.09%, and 0.24% when agricultural land above a 25° slope, agricultural land above a 15° slope, and all agricultural land were converted to forestland, respectively. The GWS was reduced by 1.18% when all forestland was converted to agricultural land (Figure 12).

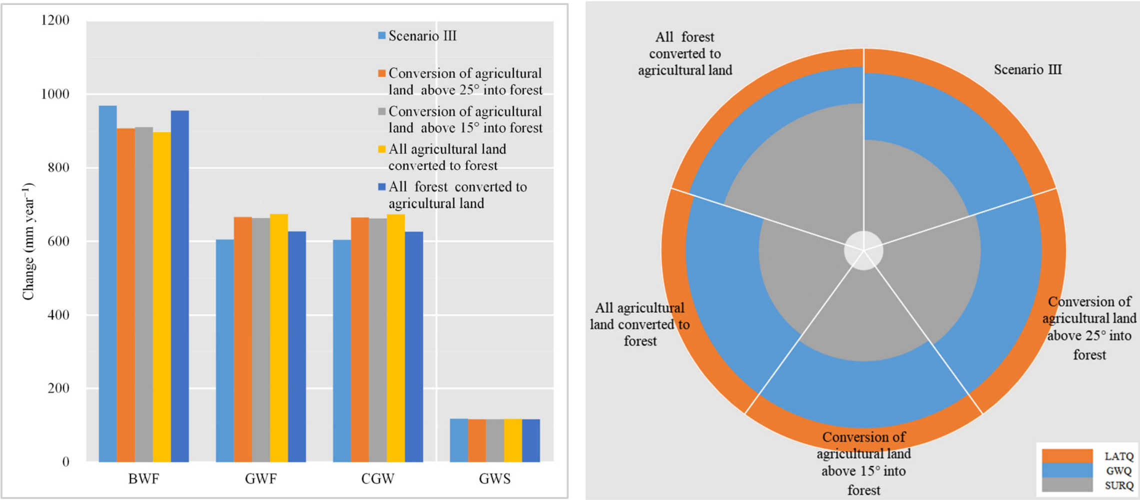

(**a**) (**b**)

Figure 12. Simulation of the annual mean values (**a**) and proportions (**b**) of BWF, GWF, green water storage (GWS), and their components in the upper Ganjiang River basin by individually altered land-use factors based on Scenario III.

4. Discussion

In the SWAT model, only the land-use data for a fixed year can be entered. This feature makes it difficult to accurately calibrate the SWAT model over a long period of time, because the simulated values, which are limited by the fixed-year land-use scenario, may deviate to some extent from the measured values, which are affected by year-to-year land-use changes. In addition, due to the model parameter uncertainty, if the simulation is carried out over an extremely long time series, the effect of long-term changes in land-use patterns on the hydrological process will be eliminated, generating pseudoparameters that will affect the accuracy of the simulation results [34]. Therefore, this study conducted scenario simulations for two separate time periods, 1980 and 2010, and the calibration and validation periods were as close to 1980 and 2010 as possible, so that the set of parameters calibrated by this simulation would be close to the actual situation without significant changes in land use during a short period. The results of the actual simulations were excellent. In the uncertainty analysis, the uncertainty in the Dongbei hydrological station simulation was larger than the uncertainty in the other station simulations; this may have been due to the presence of a reservoir near the station. Due to a lack of available data, this study did not take into account the artificial intervention from the reservoir.

Under the influence of the major factors of climate change, blue water resources have declined in the upper Ganjiang River basin over the past decades, and green water resources have increased. However, dramatic changes in land-use patterns in local areas have also had a significant impact on local blue and green water resources on the small-watershed scale. Urban construction and development processes inevitably produce a significant amount of ground compaction and soil permeability loss. These impacts result in increased surface runoff and a significantly reduced amount of water that reaches unsaturated soils, which facilitates the transition of green water into blue water [35]. In the two studied periods of land-use change, the area of forested land in the upper Ganjiang River basin changed little or even decreased. In fact, from 1980 to 2010, natural restoration and artificial interventions (such as large-scale afforestation) in the upper reaches of the Ganjiang River significantly increased the vegetation cover in the region [23,36]. Theoretically, vegetation restoration will increase the soil moisture to some extent, thus increasing the green water [37]. However, our simulation results do not support this conclusion. This is mainly because in this study, when performing simulations in SWAT, only the effect of land-use change on the regional water cycle was considered, and it was assumed that the vegetation cover was uniform within the same land-use type. This assumption ignores the effects of changes in vegetation cover on the regional water cycle within the same land-use type, which may have led to some deviations from the simulation results.

The comparison of the different precipitation and temperature scenarios showed that precipitation significantly amplifies the changes in BWF. This is because the amount of water that can be stored in the soil and vegetation is not infinite; as precipitation increases, the soil and vegetation become saturated with water, and any additional precipitation cannot be absorbed. According to the water balance principle, this part of the precipitation is directly transformed into blue water, resulting in an increase in the proportion of blue water that is greater than the increase in precipitation. Especially in wet regions, this trend may be more pronounced due to the high soil moisture content. Similarly, when precipitation decreases, the water entering the soil preferentially replaces the water consumed by the soil and plants, leading to further reductions in the BWF. In this process, surface runoff, which is directly affected, responds more sensitively to precipitation than to GWQ and LATQ. Higher temperatures will lead to increased evaporation and a corresponding reduction in BWF. Interconversions between forests and agricultural land also cause interconversions between blue and green water. When the amount of forestland increases, more precipitation is retained, which affects the surface water processes in the catchment. Some of the blue water is absorbed by plants and soil and is converted to green water through evapotranspiration, resulting in a decrease in BWF and an increase in GWF. The reduction in the total blue water volume resulting from the conversion of all forestland to agricultural land was not significant. However, due to the reduced capacity of the land to retain soil and water, precipitation tends to be "lost" rather than "stored", which leads to an increase in surface production sinks and evapotranspiration and a corresponding decrease in GWQ and LATQ [38].

In fact, the SWAT model can only simplistically describe theoretical hydrological cycle processes, and it is difficult to fully explain the complex interconversion processes that occur between blue water and green water [39]. In addition, this study has some limitations due to the limitations on data collection. First, this study uses only flow data from river hydrological stations to calibrate and validate the model, but it does not include actual the evapotranspiration and soil moisture in the model calibration. Second, the effects of reservoirs on the hydrological cycle were not considered in the simulation process. These factors affect the results of the simulations to some extent and need to be addressed in future studies.

5. Conclusions

In this study, the effects of climate and land-use change on blue water flow (BWF), green water flow (GWF), and green water storage (GWS) and their components were quantitatively analyzed with the SWAT model for different scenarios in the upper reaches of the Ganjiang River basin, which is a humid region in southeastern China. The conclusions can be summarized in the following four points.

(1) Between the 1980s and 2010s, the BWF decreased by 86.03 mm year^{-1}, the GWF increased by 8.61 mm year^{-1}, and the GWS increased by 12.51 mm year^{-1} in the upper Ganjiang River basin under the combined influence of climate and land-use change. Climate change decreased the components of BWF and increased the components of GWF. Land-use change slightly decreased the BWF components surface runoff (SURQ) and groundwater flow (GWQ), slightly increased the lateral flow (LATQ), slightly decreased the consumed green water (CGW) in the GWF, and slightly decreased the GWS. Climate change has a stronger influence than land-use change on blue and green water in the upper Ganjiang River basin.

(2) In terms of spatial distribution, the BWF was overrepresented around the basin and underrepresented in the center. The BWF tended to increase in the northern part of the basin and decrease in the southern part of the basin, while the GWF was low in the southeastern part and high in the northwestern part. Climate change increased the GWF in the eastern and northwestern parts of the basin and decreased GWF in the central part and some of the

southwestern part. GWS was positively correlated with regional elevation and showed slightly greater increases in the northeast, southwest, and west than in the other regions. For land-use change, conversions between built-up and non-built-up land uses resulted in large changes in blue-green water resources in local areas but did not have an overall impact.

(3) The trend in the BWF was consistent with that in precipitation, and changes in precipitation significantly augmented the changes in BWF. When precipitation increased by 10%, 20%, and 30%, BWF increased by 9.81%, 25.41%, and 41.5%, respectively; when precipitation decreased by 10%, 20%, and 30%, BWF decreased by 21.41%, 36.92%, and 51.74%, respectively. The proportion of SURQ in the BWF was positively correlated with changes in precipitation, and the proportion of LATQ was negatively correlated with changes in precipitation. The changes in GWF and CGW were consistent with increasing and decreasing trends in precipitation. The increase in temperature led to an increase in GWF and a decrease in BWF, both of which were most sensitive to the temperature increase of up to 1 °C. The GWS also showed a slight decreasing trend with increasing temperature.

(4) All agricultural land and forests conversion scenarios resulted in a decrease in BWF and an increase in GWF in the watershed. When agricultural land above 25°, agricultural land above 15°, and all agricultural land were converted to forestland, the BWF in the upper Ganjiang River basin decreased by 6.4%, 6.08%, and 7.44%, the GWF increased by 10.14%, 9.7%, and 11.48%, and the GWS decreased by 1.22%, 1.09%, and 0.24%, respectively. When all forestland was converted to agricultural land, the GWF increased by 3.68% and the BWF decreased by 1.45%, but the proportion of SURQ increased rapidly from 51% in Scenario III to 72%.

This study provides a useful direction for further refining the study of blue and green water. However, there are still some areas that need improvement. The role of the land-use changes on blue and green water must be more deeply explored. For example, the construction of reservoirs and factors of change inside forests (e.g., vegetation cover) need to be considered. In addition, there is a need to continue to optimize model parameters to improve the accuracy and scientific validity of simulations.

Author Contributions: Y.Z. performed the data compilation, simulations, analysis, and drafted the manuscript. C.T. and S.Z. contributed to the conception of the study. S.Z. and A.Y. helped revised the manuscript. X.N. and A.T. assisted in the SWAT model calculation. T.Z. and H.Z. made contributions in reviewing and editing the manuscript. All authors have read and agreed to the published version of the manuscript.

Funding: This research was jointly funded by the National Key Research and Development Program of China (2018YFC0407602, 2019YFC1510503), the National Natural Science Foundation of China (No. 41867016)), the Natural Science Foundation of Jiangxi Province (20202BABL203029), and the Water Conservancy Science and Technology Project of Jiangxi Province (No. 201821ZDKT15, KT201716, KT201616, 201821ZDKT18).

Acknowledgments: We are very grateful to Haijin Zheng, Yuejun Song and Kaitao Liao for providing data, and their support for this paper.

Conflicts of Interest: The authors declare no conflict of interest.

References

1. Jiang, T.; Chen, Y.D.; Xu, C.-Y.; Chen, X.; Chen, X.; Singh, V.P. Comparison of hydrological impacts of climate change simulated by six hydrological models in the Dongjiang Basin, South China. *J. Hydrol.* **2007**, *336*, 316–333. [CrossRef]
2. Duan, W.; Chen, Y.; Zou, S.; Nover, D. Managing the water-climate- food nexus for sustainable development in Turkmenistan. *J. Clean Prod.* **2019**, *220*, 212–224. [CrossRef]
3. Piao, S.; Ciais, P.; Huang, Y.; Shen, Z.; Peng, S.; Li, J.; Zhou, L.; Liu, H.; Ma, Y.; Ding, Y.; et al. The impacts of climate change on water resources and agriculture in China. *Nature* **2010**, *467*, 43–51. [CrossRef] [PubMed]
4. Zhou, F.; Xu, Y.; Chen, Y.; Xu, C.Y.; Gao, Y.; Du, J. Hydrological response to urbanization at different spatio-temporal scales simulated by coupling of CLUE-S and the SWAT model in the Yangtze River Delta region. *J. Hydrol.* **2013**, *485*, 113–125. [CrossRef]

5. Aronica, G.; Cannarozzo, M. Studying the hydrological response of urban catchments using a semi-distributed linear non-linear model. *J. Hydrol.* **2000**, *238*, 35–43. [CrossRef]
6. Bussettini, M. Environmental Flows in Sustainable Integrated Water Resources Management. *WMO Bull.* **2018**, *67*, 65–67.
7. Zang, C.; Liu, J. Trend analysis for the flows of green and blue water in the Heihe River basin, northwestern China. *J. Hydrol.* **2013**, *502*, 27–36. [CrossRef]
8. Zhao, A.; Zhu, X.; Liu, X.; Pan, Y.; Zuo, D. Impacts of land use change and climate variability on green and blue water resources in the Weihe River Basin of northwest China. *Catena* **2016**, *137*, 318–327. [CrossRef]
9. Yuan, Z.; Xu, J.; Meng, X.; Wang, Y.; Yan, B.; Hong, X. Impact of Climate Variability on Blue and Green Water Flows in the Erhai Lake Basin of Southwest China. *Water* **2019**, *11*, 424. [CrossRef]
10. Zang, C.; Mao, G. A Spatial and Temporal Study of the Green and Blue Water Flow Distribution in Typical Ecosystems and its Ecosystem Services Function in an Arid Basin. *Water* **2019**, *11*, 97. [CrossRef]
11. Falkenmark, M.; Rockström, J. The New Blue and Green Water Paradigm: Breaking New Ground for Water Resources Planning and Management. *J. Water Resour. Plan. Manag.* **2006**, *132*, 129–132. [CrossRef]
12. Yuan, Z.; Xu, J.; Wang, Y. Historical and future changes of blue water and green water resources in the Yangtze River source region, China. *Theor. Appl. Climatol.* **2019**, *138*, 1035–1047. [CrossRef]
13. Zuo, D.; Xu, Z.; Peng, D.; Song, J.; Cheng, L.; Wei, S.; Abbaspour, K.C.; Yang, H. Simulating spatiotemporal variability of blue and green water resources availability with uncertainty analysis. *Hydrol. Process.* **2015**, *29*, 1942–1955. [CrossRef]
14. Falkenmark, M. Land-water linkages: A synopsis. *Fao Land Water Bull.* **1995**, *1*, 15–16.
15. Rockström, J.; Falkenmark, M.; Allan, T.; Folke, C.; Gordon, L.; Jägerskog, A.; Kummu, M.; Lannerstad, M.; Meybeck, M.; Molden, D.; et al. The unfolding water drama in the Anthropocene: Towards a resilience based perspective on water for global sustainability. *Ecohydrology* **2014**, *7*, 1249–1261. [CrossRef]
16. Gassman, P.; Reyes, M.; Green, C.; Arnold, J. The soil and water assessment tool: Historical development, applications, and future research directions. *Trans. Asabe* **2007**, *50*, 1211–1250. [CrossRef]
17. Zang, C.F.; Liu, J.; van der Velde, M.; Kraxner, F. Assessment of spatial and temporal patterns of green and blue water flows under natural conditions in inland river basins in Northwest China. *Hydrol. Earth Syst. Sci.* **2012**, *16*, 2859–2870. [CrossRef]
18. Duncan, A. World agriculture: Towards 2010. *Food Policy* **1997**, *22*, 101–103. [CrossRef]
19. Zhu, K.; Xie, Z.; Zhao, Y.; Lu, F.; Song, X.; Li, L.; Song, X. The Assessment of Green Water Based on the SWAT Model: A Case Study in the Hai River Basin, China. *Water* **2018**, *10*, 798. [CrossRef]
20. Zeng, Z.; Liu, J.; Koeneman, P.H.; Zarate, E.; Hoekstra, A.Y. Assessing water footprint at river basin level: A case study for the Heihe River Basin in northwest China. *Hydrol. Earth Syst. Sci.* **2012**, *16*, 2771–2781. [CrossRef]
21. Chapagain, A.K.; Hoekstra, A.Y.; Savenije, H.H.G.; Gautam, R. The water footprint of cotton consumption: An assessment of the impact of worldwide consumption of cotton products on the water resources in the cotton producing countries. *Ecol. Econ.* **2006**, *60*, 186–203. [CrossRef]
22. Wan, Z.W.; Chen, X.; Ju, M.; Ling, C.H.; Liu, G.X.; Lin, S.P.; Liu, H.H.; Jia, Y.L.; Jiang, M.X.; Liao, F.Q. Streamflow Reconstruction and Variation Characteristic Analysis of the Ganjiang River in China for the Past 515 Years. *Sustainability* **2020**, *12*, 1168. [CrossRef]
23. Guo, L.P.; Mu, X.M.; Hu, J.M.; Gao, P.; Zhang, Y.F.; Liao, K.T.; Bai, H.; Chen, X.L.; Song, Y.J.; Jin, N.; et al. Assessing Impacts of Climate Change and Human Activities on Streamflow and Sediment Discharge in the Ganjiang River Basin (1964–2013). *Water* **2019**, *11*, 1679. [CrossRef]
24. Guo, L.-P.; Yu, Q.; Gao, P.; Nie, X.-F.; Liao, K.-T.; Chen, X.-L.; Hu, J.-M.; Mu, X.-M. Trend and Change-Point Analysis of Streamflow and Sediment Discharge of the Gongshui River in China during the Last 60 Years. *Water* **2018**, *10*, 1273. [CrossRef]
25. Yu, H.Y.; Li, F.B.; Liu, C.S.; Huang, W.; Liu, T.X.; Yu, W.M. Iron Redox Cycling Coupled to Transformation and Immobilization of Heavy Metals: Implications for Paddy Rice Safety in the Red Soil of South China. In *Advances in Agronomy*; Sparks, D.L., Ed.; Elsevier: Amsterdam, The Netherlands, 2016; Volume 137, pp. 279–317.
26. Torabi Haghighi, A.; Darabi, H.; Shahedi, K.; Solaimani, K.; Kløve, B. A Scenario-Based Approach for Assessing the Hydrological Impacts of Land Use and Climate Change in the Marboreh Watershed, Iran. *Environ. Modeling Assess.* **2019**, *25*, 41–57. [CrossRef]

27. Shi, P.; Zhang, Y.; Ren, Z.; Yu, Y.; Li, P.; Gong, J. Land-use changes and check dams reducing runoff and sediment yield on the Loess Plateau of China. *Sci. Total Environ.* **2019**, *664*, 984–994. [CrossRef]
28. Guzha, A.C.; Rufino, M.C.; Okoth, S.; Jacobs, S.; Nóbrega, R.L.B. Impacts of land use and land cover change on surface runoff, discharge and low flows: Evidence from East Africa. *J. Hydrol. Reg. Stud.* **2018**, *15*, 49–67. [CrossRef]
29. Abbaspour, K.C.; Rouholahnejad, E.; Vaghefi, S.; Srinivasan, R.; Yang, H.; Kløve, B. A continental-scale hydrology and water quality model for Europe: Calibration and uncertainty of a high-resolution large-scale SWAT model. *J. Hydrol.* **2015**, *524*, 733–752. [CrossRef]
30. Douglas-Mankin, K.R.; Srinivasan, R.; Arnold, J.G. Soil And Water Assessment Tool (Swat) Model: Current Developments And Applications. *Trans. Asabe* **2010**, *53*, 1423–1431. [CrossRef]
31. Arnold, J.G.; Moriasi, D.N.; Gassman, P.W.; Abbaspour, K.C.; White, M.J.; Srinivasan, R.; Santhi, C.; Harmel, R.D.; van Griensven, A.; Liew, M.W.V.; et al. SWAT: Model Use, Calibration, and Validation. *Trans. ASABE* **2012**, *55*, 1491–1508. [CrossRef]
32. Abbaspour, K.; Vejdani, M.; Haghighat, S. SWAT-CUP calibration and uncertainty programs for SWAT. *Proc. Intl. Congr. Model. Simul. (Modsim'07)* **2007**, *364*, 1596–1602.
33. Gupta, H.; Kling, H.; Yilmaz, K.; Martinez, G. Decomposition of the Mean Squared Error and NSE Performance Criteria: Implications for Improving Hydrological Modelling. *J. Hydrol.* **2009**, *377*, 80–91. [CrossRef]
34. Feng, C.; Mao, D.; Zhou, H.; Cao, Y.; Hu, G. Impacts of climate and land use changes on runoff in the Lianshui basin. *J. Glaciol. Geocryol.* **2017**, *39*, 395–406.
35. Jiang, L.; Gerten, D.; Liu, J.; Zang, C. Influence of human activities and climate variability on green and blue water provision in the Heihe River Basin, NW China. *J. Water Clim. Chang.* **2015**, *6*, 800–815. [CrossRef]
36. Zheng, H.; Fang, S.; Yang, J.; Xie, S.; Chen, X. Analysis on Evolution Characteristics and Impacting Factors of Annual Runoff and Sediment in the Ganjiang River During 1970–2009. *J. Soil Water Conserv.* **2012**, *26*, 28–32.
37. Zhao, H.; He, H.; Wang, J.; Bai, C.; Zhang, C. Vegetation Restoration and Its Environmental Effects on the Loess Plateau. *Sustainability* **2018**, *10*, 4676. [CrossRef]
38. Emmett, A.J.J.; Barron, J.N.; Veall, N. The use of I131 albumin tissue clearance measurements and other physiological tests for the clinical assessment of patients with lymphœdema. *Br. J. Plast. Surg.* **1967**, *20*, 1–15. [CrossRef]
39. Kiniry, J.; Williams, J.; Srinivasan, R. *Soil and Water Assessment Tool User's Manual*; Texas Water Resources Institute, USDA Agricultural Research Service: College Station, TX, USA, 2000; Volume 202.